Modeling of a Piezo Paddle Micro Pump

Ingo Ederer

Lehrstuhl für Feingeraetebau und Mikrotechnik
Technical University of Munich, Germany
ingo@mail.fgb.mw.tu-muenchen.de

ABSTRACT

In this paper an analytical method will be presented to describe the behavior of a piezo electric paddle pump. For that, mechanical and fluidic mechanism are combined in a one mass oscillator model with fluidic damping. With that model it is possible to simulate the complete droplet ejection process. It is also possible to optimize the shape of the actuator, the number of nozzles, the location of the nozzles and the shape of the pump chamber. As a result, the simulation will be compared with the measurements of a real droplet generator. Additional design rules for such a micro pump will be given.

Keywords: micro pump, droplet generator, piezoelectric bender actuator, analytical description

INTRODUCTION

Droplet generators based on piezoelectric bender actuators are known since the early 70's [2]. However this technique will get more attractive this time due to improved piezo ceramics. Last year a droplet generator developed at the Lehrstuhl für Feingerätebau was presented to provide a adjustable amount of atomized liquid i.e. for fuel in a heater [7]. With such a droplet generator 10 ml/min can be atomized out of 67 nozzles. At the same time the dimensions of this pump are 9x15x8 mm³.

FUNCTION PRINCIPLE

The function principle is similar to common piezoelectric printheads: a piezoelectric element changes the volume of a pump chamber. This induces the droplet ejection through a variety of nozzles. In this case a piezoelectric bender actuator is mounted in small distance to a nozzle plate inside of a pump chamber filled with the working fluid (see figure 1 and figure 2).
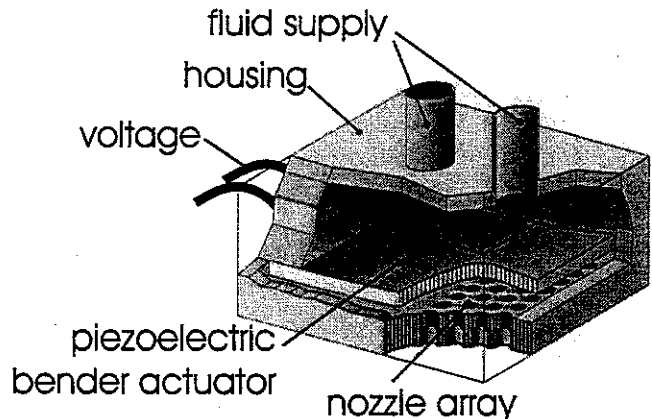

Figure 1: Cross-sectional view of a piezoelectric droplet generator

Following a suitable voltage pulse, the bender (paddle) is flexed away relatively slowly from the nozzles. The capillary pressure of the liquid-solid-gas interface in the nozzles causes a fuel flow from the supply system into the chamber. The fuel-air interface near the output port of the nozzles assumes a concave shape, the so-called meniscus. The surrounding fluid fills up the gap between bender actuator and nozzle plate. Then the mechanical tension is released instantaneously by shorting the electrodes of the piezo layers. The sudden motion of the paddle towards the nozzles causes the fluid to be squeezed through, resulting in drop ejection analogous to ink-jet printhead systems (see figure 2).
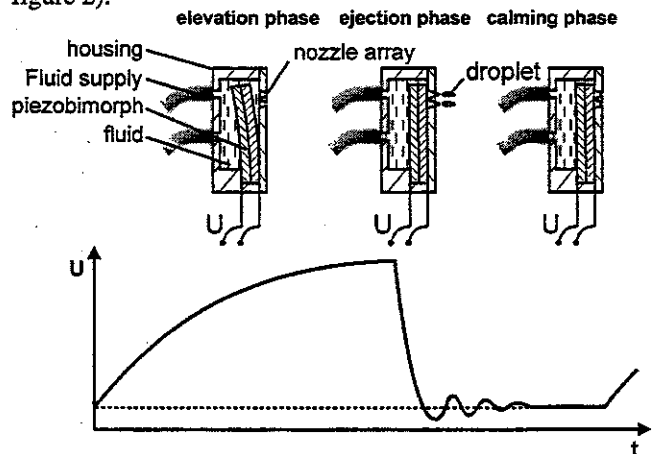

Figure 2: function scheme

By supplying a multitude of tiny nozzles (nozzle diameter: 50 microns) from a single paddle, a very good performance as well as cost to performance ratio is achieved. Other advantages are the insensitivity against air bubbles inside the pump chamber and the possibility to control the liquid flow by changing the frequency.

OBJECTIVES

Several questions should be answered by the modeling:
- the maximum pressure inside the pump
- the droplet mass and velocity
- location of the nozzle
- several optimized dimensions like the remaining gap size between paddle and nozzle plate

PIEZOELECTRIC ACTUATOR

In this micro pump a piezo bimorph is used for actuation. The upper layer is active and laminated as multilayer to reduce the voltage. The static elevation of the piezo tip can be calculated as [1]:

$$Y_{max} = \frac{3 \cdot d_{31} \cdot E_{el} \cdot l_{piezo}^2}{4 h_{piezo}} \tag{1}$$

The first natural bending frequency:

$$f_1 = \frac{1,875^2}{2 \cdot \pi} \cdot \sqrt{\frac{h_{piezo}^2}{12 \cdot \rho \cdot l^4 s_{11}}} \tag{2}$$

The electrical behavior of the actuator can be described as a capacitance C with an additional loss. The circuit is shown in the figure below.

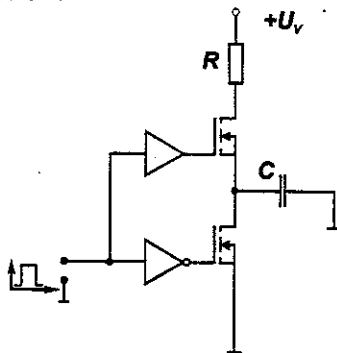

Figure 3: electrical cicuit

Corresponding to the charge curve of the capacitance the piezo voltage can be calculated as:

$$U_p(t) = \begin{cases} U_{max}\left(1 - e^{-\frac{t}{R \cdot C}}\right), & \text{for } 0 \leq t \leq t_{on} \\ 0, & \text{for } t < 0 \vee t > t_{on} \end{cases} \tag{3}$$

FLUIDMECHANICAL MODELLING
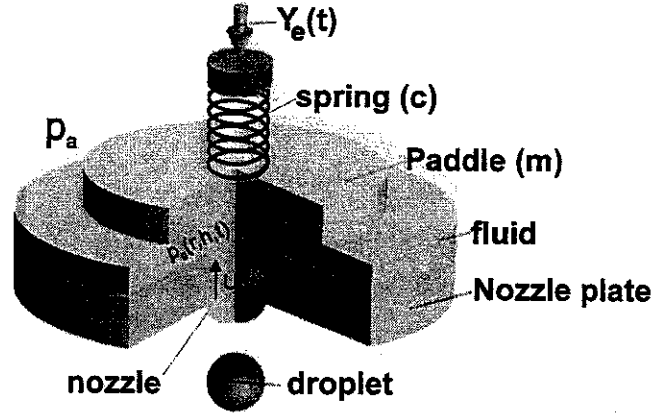
Figure 4: schematic view of the model

For getting results immediately about tendencies of the effect of several parameters, an analytical view is preferred. The most simple way for modeling the droplet generator is to use an one mass oscillator model. In this model the actuator is the oscillating mass. Its stiffness is modeled by the spring as shown in figure 4. The damping comes from the fluid which is squeezed through the gap between actuator and nozzle plate and through the nozzles while oscillating. Due to the small elevation of the piezo bender compared to the beam length, it can be assumed that the gap is parallel during oscillation. Another simplification is the concentric modeling of the pump. One nozzle is placed in the center of the model. In case other nozzles can be added on a concentric circle in a certain distance to the center. The system can be stimulated by applying a length distortion on the free spring. The electrical feedback from the piezo ceramic and with that hystereses effects could be neglected because of the oscillation. The connection between mechanical and fluid systems comes from the damping force F_d. The inner damping of the piezo actuator can be neglected in comparison to the fluidic force.

Figure 5: names and numbers of the model

With that, the system describing differential equation can be given as:

$$m_p \cdot \ddot{h} = c \cdot (h - h_0 + Y_E) + F_d \qquad (4)$$

The system stiffness c can be calculated as

$$c = (2\pi \cdot f_I)^2 \cdot m_p \qquad (5)$$

The excitation function $Y_E(t)$ follows the piezo-electrical behavior of the actuator:

$$Y_E(t) = Y_{max} \cdot \frac{U_p}{U_{max}} \qquad (6)$$

In the gap, a flat laminar flow with a parabolic velocity profile can be assumed. This applies also for the laminar tube flow in the nozzle. The pressure outside the gap and at the nozzle exit is equal to the surrounding pressure and can be set to zero. The damping force F_d can be calculated due to the integration of the pressure along the complete gap area:

$$F_d = \int_{0}^{2\pi} \int_{r_d}^{r_a} r \cdot p_g \cdot dr \cdot d\varphi + \int_{0}^{2\pi} \int_{0}^{r_d} r \cdot p_I \cdot dr \cdot d\varphi \qquad (4)$$

The gap pressure results from the solution of Navier-Stokes differential equation in cylindrical coordinates:

$$\frac{dU_g}{dt} = -\frac{1}{\rho} \frac{\partial p}{\partial r} + \frac{\eta}{\rho} \left(\begin{array}{c} \frac{1}{r} \frac{\partial}{\partial r} \left(r \frac{\partial U_g}{\partial r} \right) + \frac{1}{r^2} \frac{\partial^2 U_g}{\partial \varphi^2} \\ + \frac{\partial^2 U_g}{\partial z^2} - \frac{2}{r^2} \frac{\partial U_g}{\partial \varphi} - \frac{U_g}{r^2} \end{array} \right) \qquad (7)$$

The gap velocity can be calculated with the condition for continuity in dependence on the nozzle velocity $U_0(t)$ and the gap height h(t):

$$\overline{U}_g(t,r) = -\frac{-r_n^2 \cdot U_0 + r_n^2 \cdot \dot{h} + r_n^2 \cdot h \cdot \dot{h}}{2r \cdot h} \qquad (8)$$

Under usage of the assumptions of a parabolic velocity shape the gap velocity can be written as:

$$U_g(t,r,z) = 6 \cdot \overline{U}_g \cdot \left(\frac{z}{h} - \frac{z^2}{h^2} \right) \qquad (9)$$

Some transformations induces to the expression for the gap pressure:

$$p_g(t,r) = p_I + \frac{1}{4h^4} \left(log \left(\frac{r}{r_d} \right) \left(\begin{array}{c} (U_0 - \dot{h}) \\ (2h \cdot \dot{h} \cdot \rho \cdot r_n^2 - 24r_n^2 \eta) \\ -2r_n^2 \rho \cdot h^2 (\dot{U}_0 - \ddot{h}) \end{array} \right) \right) +$$
$$\frac{1}{4h^4} (r_n^2 - r^2)(12h \cdot \dot{h} \cdot \eta + \rho \cdot h^3 \cdot \ddot{h}) \qquad (10)$$

The pressure above the nozzle entry $p_1(t)$ can be derived from Hagen Poisseuille's equation for the unsteady flow in a tube:

$$\dot{U}_0(t) = -\frac{3}{4\rho} \frac{p_I - p_c}{l_n} - \frac{6\eta \cdot U_0}{\rho \cdot r_n^2} \qquad (11)$$

In this equation the capillary pressure $p_c(t)$ is unknown. For calculating this, a simply interfacial tension model will be generated. It will be assumed that the shape of the interfacial between fluid and the surrounding air is always spherical. The minimum radius is given through the nozzle radius r_n. A further ejection of fluid leads to a semi sphere followed by a fluid cylinder with the nozzle radius. For the calculation of the capillary pressure first of all the liquid level s_n will be determined, after that that the sphere radius r_c can be calculated. The calculation is divided into three areas:

for $s_n < -\frac{2}{3} r_n$ is: $r_c = r_n$

for $s_n > \frac{2}{3} r_n$ is: $r_c = -r_n$

for $-\frac{2}{3} r_n \leq s_n \leq \frac{2}{3} r_n$ is:

514

$$r_c = \frac{r_n^2}{12 \cdot s_n} + \frac{0.31498 \cdot r_n^3}{s_n \cdot z} +$$
$$\frac{0.02205 \cdot r_n \cdot z}{s_n}, \text{ with} \quad (12)$$

$$z = \left(\frac{54 r_n^3 - \frac{3888}{r_n^2} s_n^2 \left(-r_n^3 - 9 s_n^2 r_n \right) +}{\frac{34992}{r_n} s_n \left(\frac{r_n^2}{18} + s_n^2 \right) \sqrt{\frac{r_n^2}{9} + s_n^2}} \right)^{\frac{1}{3}}$$

The capillary pressure:

$$p_c(t) = \frac{\sigma}{r_k} \quad (13)$$

For modeling the droplet separation, a simply criteria will be defined. Two conditions shall be fulfilled: First, the liquid level has to be outside of the nozzle tip in a certain amount. Second, coming from a negative value, a zero crossing in the nozzle speed should happen. After the droplet separation, the new liquid level is at the nozzle tip. The liquid movement in the nozzle continues with the same start value as before (see figure 6).

$$dl < l_n - 2/3\, r_n \qquad l_n - 2/3\, r_n < dl \le l_n \qquad l_n < dl \le l_n + 2/3\, r_n$$

$$l_n + 2/3\, r_n < dl \qquad l_n + 2/3\, r_n < dl \wedge u_0 < 0 \qquad dl = l_n$$
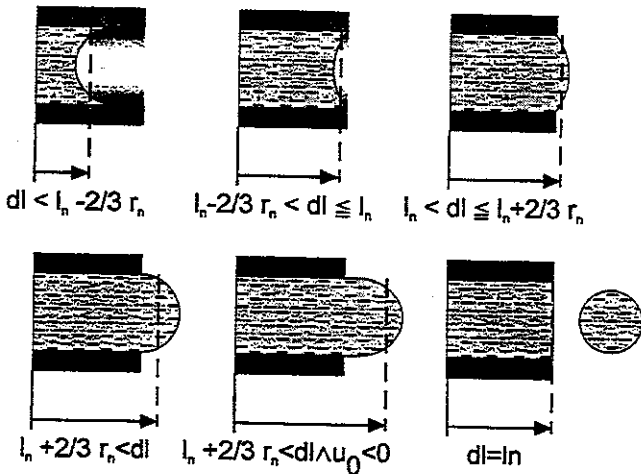
Figure 6: drop pull off model

Thus, the droplet separation can be modeled as a discontinuity in the solution of the differential equation system. The system looses some liquid to a discrete point in time. This loss in mass induces a changed impulse balance in the further calculation. Due to, a new start of the calculation at the time point t_0 with new boundary conditions is necessary. These boundary conditions are the paddle level $h(t)$ the paddle velocity $\dot{h}(t)$ and the liquid velocity $U_0(t)$ which will be calculated at the time point before the droplet tear off. With these values and the new liquid level $s_n(t_0) = 0$ a new calculation run can be started.

$$h(t_o) = h(t_{o-1}), \dot{h}(t_o) = \dot{h}(t_{o-1}),$$
$$U_0(t_o) = U_0(t_{o-1}), s_n(t_o) = 0 \quad (14)$$

With the condition:

$$\dot{s}_n = U_0 \quad (15)$$

the boundary condition:

$$p_g(r_a, t) = 0 \quad (16)$$

and (4), three equations are available, which can be solved numerical.

RESULTS

The following graphs are showing the calculation results with the data set given below.

paddle radius	250	μm
paddle mass	9.55×10^{-7}	kg
paddle stiffness	5.97	N/mm
1. natural bending frequency	12.5	kHz
max. elevation	12	μm
excitation frequency	1	kHz
nozzle diameter	20	μm
residual gap	19	μm
fluid viscosity	8	mPa s
fluid surface tension	73	mN/m

The computation period goes over 3 cycles from 0 s to 0.003 s. The solution is approximated with 10000 steps, which takes 12 minutes on a Pentium 233 processor.
Figure 7 shows the numerical result of the paddle elevation in comparison to the measurement of the piezo bending at the tip of a real system, measured during operation.
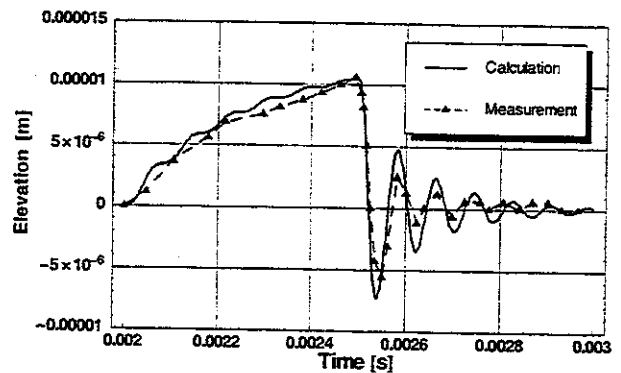

Figure 7: elevation of the piezo tip versus time

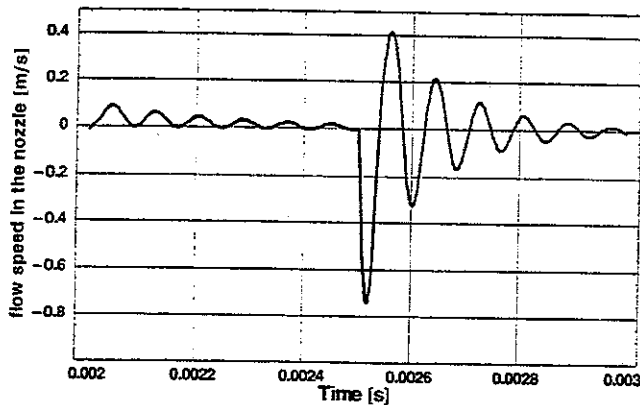The calculated nozzle velocity $U_0(t)$ is shown in the next graph:

Figure 8: nozzle velocity versus time

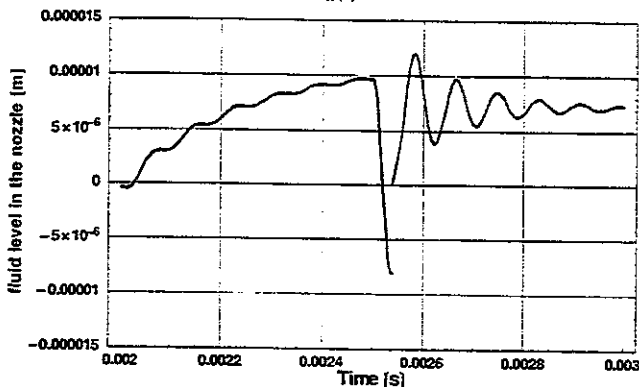The fluid level in the nozzle $s_n(t)$:

Figure 9: fluid level versus time

In Figure 9 the discontinuity at the time 2.5 ms can be detected, which comes from the droplet separation at that point of time.

The calculated drop volume is 2.5 pl, the drop diameter is 17 μm, which is about 15 % smaller than the measured value.

Figure 10 shows the gap pressure versus time and radius.

CONCLUSION

Simulation and measurement are corresponding quite good. A calculation run goes relatively fast, that allows a parameter optimization. First results are showing that a high resonance frequency of the piezo paddle leads to a good drop pull off because of a high acceleration in the nozzle. Also high pressure over the nozzle entry is good for the drop ejection. For that, the gap shouldn't be too small to keep the damping forces down. Additional a minimum size of the paddle will be expected. On the other hand, a big gap in the range of 40 μm leads to small damping forces. The

paddle oscillation decays very slowly, and with that the shooting frequency slows down.

Next steps will go to a model with a nozzle array to see the inference of these.
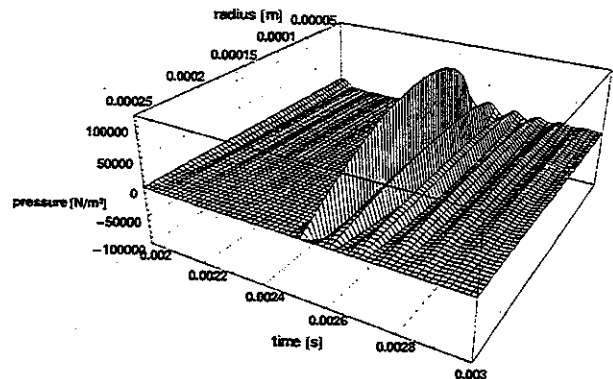

Figure 10: gap pressure versus time and radius

REFERENCES

[1] Wissenschaftliche Schriftenreihe der Technischen Hochschule Karl-Marx-Stadt: PIEZOELEKTRISCHE LINEARE STELLANTRIEBE, VEB Kongreß- und Werbedruck, Oberlungwitz 1982

[2] Elmquist, R.: RECORDER OPERATING WITH DROPS OF LIQUID, US Patent 4,072,959, 1976

[3] Berchtold A.: OPTIMIZATION OF A DROP-ON-DEMAND PRINT HEAD WITH PLANAR PIEZOCERAMIC TRANSDUCERS, SID Symposium, Las Vegas 1990

[4] Rosenstock G.: ERZEUGUNG SCHNELL FLIEGENDER TROPFEN FÜR TINTENDRUCKER MIT HILFE VON DRUCKWELLEN, Diss. TU München 1982

[5] Ederer I., Raetsch P., Schullerus W., Tille C., Zech U.: PIEZOELECTRICALLY DRIVEN MICROPUMP FOR ON-DEMAND FUEL DROP GENERATION IN AN AUTOMOBILE HEATER WITH CONTINOUSLY ADJUSTABLE POWER OUTPUT, EUROSENSOR X, Leuven 1996

[6] Ederer I., Mühlbauer W., Schullerus W., Tille C., Zollner A.: INK-JET PRINTHEADS AS MICRODOSING PUMPS: PROPERTIES AND APPLICATIONS, Eletrochemical Microsystem Technologies '96; Grevenbroich

[7] Ederer I.; Grasegger J.; Tille C.: DROPLET GENERATOR WITH EXTRAORDINARY HIGH FLOW RATE AND WIDE OPERATING RANGE. Transducer'97, Chicago. Conference Proceedings, 3A3.03. S. 809-812. IEEE 1997.